DURABILITY AND STEEL CORROSION RESISTANCE OF SLAG WITH METAKAOLIN BASED GEOPOLYMER CONCRETE

H. E. E. FOUAD[1], W. H. SOUFI[2], A. S. ELMANNAEY[3],
M. ABD-EL-AZIZ[4] AND H. EL-GHAZALY[4]

ABSTRACT

In this research, the performance of slag with metakaolin based geopolymer concrete in aggressive media is investigated. Firstly, the effect of adding metakaolin on the compressive strength of slag based geopolymer mortar is studied. Ordinary Portland cement and geopolymer concrete samples are then prepared and cured in water for 28 days then immersed in tap water and in an aggressive media for 90 days. The durability of samples is assessed using compression test, Fourier Transform Infrared Spectroscopy and Scanning Electron Microscopy. Also, Linear Polarization Resistance technique is utilized to assess the corrosion rate of steel embedded in concrete samples. It is concluded that replacing slag by 5% metakaolin by weight leads to the highest compressive strength. The compressive strength of geopolymer in aggressive media boosts by up to 30% compared to tap water. Also, the corrosion rate of steel in geopolymer samples nearly diminishes in different media. Moreover, the microstructure of geopolymer matrix shows more stable behavior in aggressive media compared to Portland cement.

KEYWORDS: Geopolymer, Slag, Meta-kaolin, Durability, Aggressive media, Steel corrosion.

1. INTRODUCTION

Recently, the world is shifting towards the use of low energy consumption products, sustainable development, and waste reuse industries [1]. Geopolymer technology is improving day after day and is going to replace Portland cement products in construction engineering [2]. The manufacturing process of geopolymer relies on

---

[1] Assistant Professor, Construction Engineering Department, Faculty of Engineering, Misr University for Science and Technology, Egypt.
[2] Professor, Building Physics and Environment Institute, Housing and Building National Research Center, Egypt.
[3] Assistant Professor, Construction Engineering Department, Faculty of Engineering, Misr University for Science and Technology, Egypt, ahmed.elmannaey@must.edu.eg.
[4] Professor, Department of Civil Engineering, Faculty of Engineering, Fayoum University, Egypt.

utilizing natural and/or industrial by-product materials (base materials) to meet the goal of sustainability and to reduce carbon dioxide emissions [3]. In spite of its promising strength and durability performance, geopolymer still needs more in depth research and advancements; i.e., the optimum mix proportions of base material, its durability and corrosion resistance [4].

Base materials are induced by adding alkaline activator solution (mainly sodium and potassium-based materials) which react with silicon (Si) and aluminum (Al) in base materials to produce geopolymer binders [5-8]. These binders are formed by dissolving Si and Al ions with the aid of the high alkalinity activator solution. These ions then coagulate in a small structure (monomer), and finally, these monomers are condensed to form hydrated products [9-12].

The effect of aggressive media on the performance of geopolymer concrete attracted researchers' attention during the last few decades. Low calcium fly ash based geopolymer samples showed high durability when exposed to high concentrations of sulfuric acid and chloride solution for 180 days. The samples lost minor weight, resisted surface erosion and kept their ultimate strength nearly unaltered. Moreover, the concrete matrix acted as nearly an impermeable material which protected the embedded steel bars from corrosion [13].

On the other hand, fly ash based geopolymer mortar specimens when immersed in 10% magnesium sulphate solution for 24 weeks showed loss of durability. The samples gained very little weight and lost more than half of their ultimate strength at the end of the study period. Also, white deposits were formed on the surface of the samples as soft deposits and converted later to hard crystals [14]. Whereas, the performance of sodium hydroxide activated copper slag based geopolymer in sulphates and chlorides aggressive solutions depicted a slight increase in the compressive strength. Moreover, the corrosion resistance of the samples was enhanced in the aggressive media [15, 16]. A supporting study also concluded that the resistance of Na_2CO_3-activated blast furnace slag cement to the corrosive solution was excellent, and that the samples prevented the corrosion of steel bars after 7 years of immersion [17].

Alkali-activated slag concrete lost less strength than Portland cement concrete after immersion in 5% Na_2SO_4 and $MgSO_4$ solutions [18]. Another study synthesized slag based geopolymer with seawater in a coastal area and revealed that the compressive strength of the specimens improved [19].

It is a common practice to add metakaolin to Portland cement to obtain concrete with lower porosity and higher durability. However, this practice is still not well studied in the field of geopolymer concrete production. Therefore, a thorough experimental study is highly needed. Also, the corrosion resistance of geopolymer concrete needs more in depth investigation to explain the mechanism of steel corrosion in geopolymer concrete.

The main purpose of this study is to investigate the effect of adding metakaolin to slag based geopolymer concrete on its compressive strength as an indicator of durability. The durability and steel corrosion resistance of the highest compressive strength geopolymer samples and Ordinary Portland Concrete samples will be tested by compression strength test, X-ray florescence (XRF), X-ray Diffraction (XRD), Fourier Transform Infrared Spectroscopy (FTIR), and Scanning Electron Microscopy (SEM) to identify the mechanical, chemical, mineralogical, and microstructural properties of geopolymer specimens. Moreover, corrosion rate of steel bars will be detected using Linear Polarization Process (LPR) technique.

2. EXPERIMENTAL

2.1 Materials

In this study, Ordinary Portland Cement (OPC), Ground Granulated Blast Furnace Slag (S) and meta-kaolin (MK) are used as cementitious materials. S is an industrial by-product material resulting from rapid cooling of molten steel and has a specific gravity of 3.52. This material is supplied by the Iron and Steel Factory, Helwan Governate, Egypt. Also, MK is used as a partial replacement for S and is obtained by calcining pure kaolin at 750°C for 2 h. Kaolin used in this study is obtained from an open quarry located in Sinai through the Middle East Mining Company (MEMCO), and

its SiO_2/Al_2O_3 molar ratio is 1.34. S and MK are grounded to obtain grain size similar to OPC with a value of 40 to75 microns.

The oxide composition of S, MK and OPC is assessed using XRF analysis and is presented in Table 1. It is obvious that S and MK are rich in siliceous and aluminous compounds but have far lower calcium composition compared to OPC. The XRD analysis of S presented in Fig. 1 shows that there are no intense peaks, but a large diffuse peak at about 20-30°, indicating that the amorphous phase is dominant in S. While, XRD of MK shows a large intense peak at about 25° with several sharp peaks that are identified as kaolinite and quartz minerals.

Table 1. Oxide composition (%weight) of the raw materials, X-ray Fluorescence (XRF) analysis.

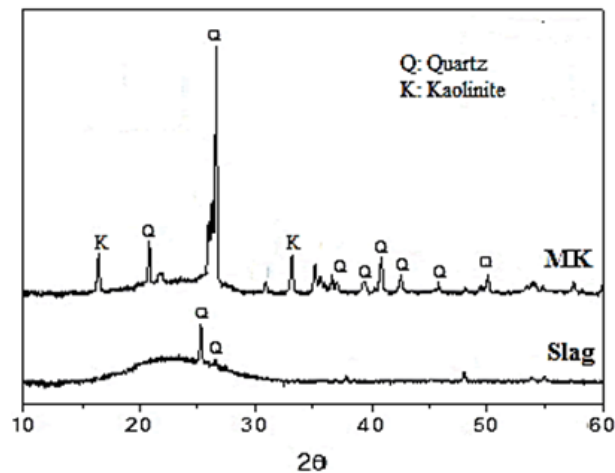| Oxide Composition	CaO	SiO$_2$	Al$_2$O$_3$	MgO	Na$_2$O	SO$_3$	Fe$_2$O$_3$	Other Oxides
OPC	64.50	21.70	6.30	1.86	0.28	1.77	3.40	0.19
S	33.07	36.59	10.01	6.43	1.39	3.52	1.48	4.88
MK	0.14	55.01	40.94	0.34	0.09	0.00	0.55	1.15

Fig. 1. XRD patterns for the base materials.

Sodium silicate, Na_2SiO_3 and sodium hydroxide, NaOH at a constant ratio of 3:1 by volume are utilized to activate the polymerization process. Na_2SiO_3 is a white viscous liquid, produced by melting sand and sodium carbonate at 1350-1450ºC under steam pressure. Its chemical composition is 8.9% Na_2O, 28.7% SiO_2 and 62.5% H_2O (by weight) with a specific gravity of 1.45. NaOH is in the form of white pellets with 99%

purity. NaOH solution is prepared at the desired molarity (12M) and kept in air for one day prior to mixing. Tap water is used throughout the synthesis process.

The aggregates used in this study are basalt and sand. Basalt has a nominal maximum particle size of 12 mm, specific gravity of 2.7, unit weight of 1.68 t/m^3 and absorption value of 0.8%. Sand has a fineness modulus of 2.6, specific gravity of 2.6, unit weight of 1.65 t/m^3, percentage of dust and fine materials of 1.4% by weight, and void ratio of 29%. The reinforcing steel is high-grade tensile carbon steel, Ezz Steel with a yield strength of 360 MPa and 12 mm in diameter.

2.2 Mix Proportions and Sample Preparation

In this study, preliminary geopolymer mortar cubes of size 7 cm are prepared with water/S ratio of 0.4 and sand/S content of 3:1 by weight. The S material is then partially replaced by MK with a replacement ratio ranging from 1 to 15% by weight as shown in Table 2, to determine the replacement ratio that results in the optimum compressive strength. OPC and S+5%MK (related to the optimum compressive strength) plain concrete cubes of size 10 cm and reinforced concrete cylinders (5cm in diameter and 10cm in height) are then synthesized with basalt: sand: binder ratio of 2:1:1 by weight and water/binder ratio of 0.47 as shown in Table 3. The cylindrical samples are reinforced by steel bars as shown in Fig. 2. It should be clear that the steel bars are initially coated by epoxy zinc primer except for two spots (of 1cm in height) that were left clear to form the closed current circuit as shown in Fig. 3.

Table 2. Preliminary mortar mixes for the current study.

Mix	OPC, g	Slag, g	MK, g	MK:Total Base Material Weight	Activator, g (ratio/binder)	Sand, g
OPC	1000	-	-	0%	400 (0.40)*	3000
S	-	1000	-	0%	400 (0.40)	3000
S+1%MK	-	990	10	1%	400 (0.40)	3000
S+3%MK	-	970	30	3%	400 (0.40)	3000
S+5%MK	-	950	50	5%	400 (0.40)	3000
S+7%MK	-	930	70	7%	400 (0.40)	3000
S+10%MK	-	900	100	10%	400 (0.40)	3000
S+15%MK	-	850	150	15%	400 (0.40)	3000

* Water

Table 3. Concrete mixes for the current study.

Mixes	OPC, kg/m^3	Slag, kg/m^3	MK, kg/m^3	Sand, kg/m^3	Basalt, kg/m^3	Water (ratio/ binder)	Activator solution (ratio/ binder)
OPC	555	-	-	555	1110	261(0.47)	-
S	-	555	-	555	1110	-	261(0.47)
S+5% MK	-	527.2	27.8	555	1110	-	261(0.47)

All the blends are mechanically mixed for 3 minutes, molded and vibrated for 30 seconds to remove entrained air. The samples are then covered with plastic wraps to avoid water evaporation and are cured at ambient temperature (T = 20 ºC ± 2 ºC, RH = 95 ± 5%) for 24 hours. After demolding, samples are cured in a water bath for 28 days. Finally, concrete samples are removed from the curing water bath and are embedded in different aggressive media; a solution of 5% sodium chloride + 5% sodium sulfate (NC-NS), a solution of 5% magnesium chloride + 5% magnesium sulfate (MC-MS) and reference samples are left in tap water (TW). The exposure period to aggressive media and tap water lasted for 90 days to assess the effect of these media on concrete mixes durability.
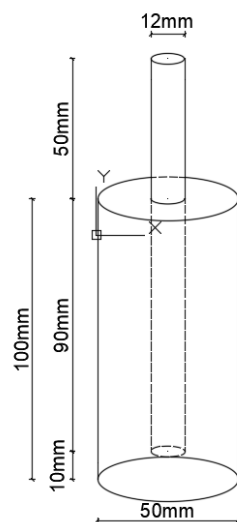

Fig. 2. Reinforcement details of concrete cylinders.

Fig. 3. Steel bars with epoxy zinc primer and uncoated spots.

2.3 Methods of Investigation

Compressive strength tests are carried out on mortar samples after 7 and 28 days and on concrete cubic samples after 7, 28, 60, and 90 days of immersion in different media. The samples are tested with a loading rate of 100 kPa/s. The crushed segments resulting from the compressive strength samples at 90 days of immersion are collected and used in FTIR and SEM tests. Perkin Elmer FTIR Spectrum RX1 Spectrometer is used to evaluate the functional groups in the sample. The samples are ground and molded with a small amount of potassium bromide and then pressed to a disk of 13 mm in diameter at a pressure of 8 t/cm^2 for FTIR analysis. The wave number ranged from 400 to 4000 cm^{-1}. The microstructure of the hardened specimens is studied using SEM Inspect S (FEI Company, Netherlands) equipped with an energy dispersive X-ray analyzer.

Steel corrosion test is conducted on the cylindrical specimens. Linear Polarization Resistance technique (LPR) is used to obtain the steel corrosion rate in accordance with ASTM C 876. The Tafel extrapolation technique is used, and the polarization experiments are carried out at a scan rate of 5mV/S.

3. RESULTS AND DISCUSSION

3.1 Compressive Strength

The compressive strength of the OPC, S, and S with MK mortar samples after 7 and 28 days, f_7 and f_c, respectively, is presented in Table 4. It is obvious that the optimum compressive strength is obtained at an MK replacement ratio of 5%. Therefore, this ratio is adopted in synthesizing concrete samples through the current research.

Table 4. Compressive strength (MPa) of mortar mixes.

Mix	OPC	S	S+1%MK	S+3%MK	S+5%MK	S+7%MK	S+10%MK
f_7	29	46.4	36.5	44.5	45.6	38.9	37.8
f_c	44.5	61	63.1	66.2	70.3	52.7	47.5

The compressive strength of the OPC, S, and S+5%MK concrete samples after curing in a water bath for 28 days (f_c) are 42.5, 56.5 and 63.3 MPa, respectively. Adding MK to S increases the compressive strength of the mix by about 12% in comparison to

S mix. This can be attributed to the availability of the ready-to-release aluminum in MK. In consequence, this affects the gaining of strength and durability. Moreover, the high silica ratio in MK results in producing higher homogeneity CSH gel [20].

The relation between the compressive strength of the hardened concrete samples and immersion time in different media (after curing in water for 28 days) is shown in Fig. 4. Immersion in TW does not affect the compressive strength much, either for OPC or S+5%MK samples. While immersion in MC-MS and NC-NS weakens the compressive strength of OPC samples (f_{90}/f_c) by about 40%. The loss of compressive strength of OPC concrete in MC-MS and NC-NS media is attributed to the sulphate attack on $Ca(OH)_2$ (CH) forming gypsum and on C_3A forming ettringite. These compounds have greater volume which results in internal stresses leading to the formation of cracks and loss of strength. Moreover, $MgSO_4$ has a detrimental effect; it attacks C-S-H, CH and C_3A and results in forming a material with no bonding abilities [21]. Also, the presence of chlorides decomposes gypsum and ettringite in the matrix to a leachable material which travels out of the concrete forming salt sediments on its surface. In consequence, the permeability of the sample increases and its strength decreases with time [21].

On the contrary, immersion of S+5%MK in MC-MS and NC-NS enhances its compressive strength (f_{90}/f_c) by about 15% and 33%, respectively. This may be attributed to the formation of more stable C-S-H gel matrix [19]. Also, the higher pace of compressive strength development with time in NC-NS compared to MC-MS is obvious. This higher rate of evolution of compressive strength in Na_2SO_4 is due to the role of sodium sulfate as an activator for slag and other cementing components [22, 23]. Also, geopolymer reaction produces an alkaline Al/Si gel which is totally different from OPC C-S-H gel, and CH formation is usually suppressed. Therefore, geopolymer generally isn't attacked by sulphates or leached by chlorides and acts as a durable material against these aggressive media [24].
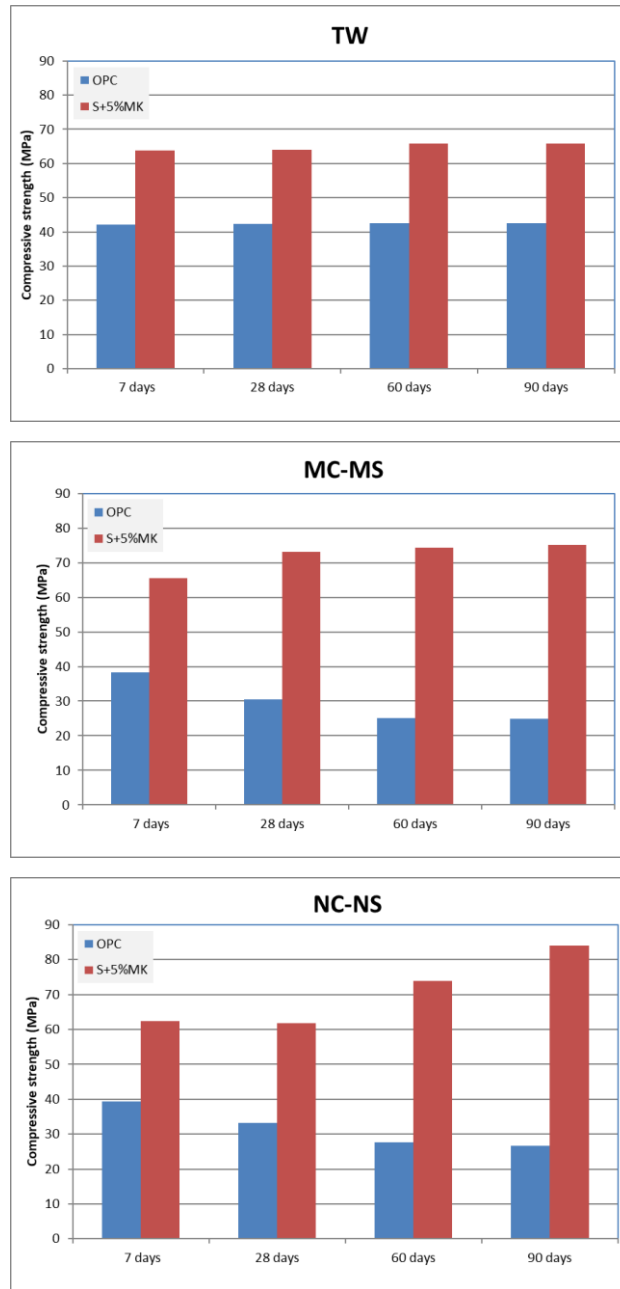
Fig. 4. Effect of immersion period in different media on concrete compressive strength.

The visual inspection conforms to the literature and the findings of the compressive strength test. Figure 5 shows the physical appearance of OPC and S+5%MK concrete samples after immersion in NC-NS and MC-MS media for 90 days. Cracks and disintegration of the edges and corners of OPC sample are obvious. Also, the salt crystals are sedimented on the specimen's surface. On the contrary, S+5%MK

sample preserved its shape and integrity. Moreover, there is a minor amount of salt sedimentations on sample's surface.

a-OPC Specimen (NC-NS)   b-S+5%MK Specimen (NC-NS)   c-S+5%MK Specimen (MC-MS)
Fig. 5. Effect of immersion in different aggressive media for 90 days on the appearance of concrete samples.

3.2 Electrochemical Behavior of Reinforcing Steel

LPR technique is used to study the protection ability of various cementing materials against steel corrosion in different media. Table 5 shows the corrosion rate (μmY^{-1}) for all samples at different time interval 7, 28, 60 and 90 days of immersion in different media.

Generally, the corrosion rate of OPC samples in different media is significantly higher than geopolymer samples. It is worth mentioning that the protection against corrosion in OPC can be achieved through two mechanisms. The first mechanism is related to the formation of the passive layer on steel surface with the aid of the high alkalinity of CH [4, 25]. The second mechanism includes the blocking role of C-S-H gel, which physically protects the steel matrix [5, 26]. The superior protection of S+5%MK samples against corrosion is due to its higher density (higher compressive strength) and a higher pH value than the OPC samples. Moreover, it possesses higher resistance to be leached by NC-NS medium or to be decomposed by MC-MS medium. The presence of slag also prohibits chloride ions from reaching the reinforcement [1, 27].

Table 5. Corrosion rate (μmY^{-1}) of reinforcement steel in different concrete samples in different aggressive media.

Mixes		7 days	28 days	60 days	90 days
TW	OPC	260	130	21	3
	S+5%MK	1.2	0.49	0.47	0.44
NC-NS	OPC	635	760	1001	630
	S+5%MK	13	11	2	0.2
MC-MS	OPC	220	250	750	1300
	S+5%MK	25	0.65	0.5	1.5

Figure 6 shows the samples which were exposed to different aggressive media for 90 days. On one hand, S+5%MK samples show the best performance as they contain very low amount of CaO. This prevents the formation of calcium carbonate. Consequently, no white deposits (salt) were formed. On the other hand, OPC samples with higher rates of CaO which react with carbon dioxide led to the appearance of calcium carbonate salts [1, 27]. It should be noted that the immersion mediums are not allowed to reach the reinforcement, therefore, the upper face of the samples are directly exposed to air.

a-OPC   b-S+5%MK (NC-NS)   c- S+5%MK (MC-MS)

Fig. 6. Photos of samples after exposure to different media for 90 days.

3.3 Microstructure of Concrete Specimens

3.3.1 Infrared analysis

IR spectroscopy can provide valuable information regarding the silicate, sulphate, and carbonate phases in the concrete matrix [28]. The infrared spectra of OPC and S+5%MK after immersion in different media for 90 days are given in Fig. 7 and

Fig. 8, respectively. In relation to OPC after comparing the spectra of OPC concrete in TW with NC-NS and MC-MS, the following observations are detected: the loss of Si-O bond in CSH gel as the band of 463 and 1031 cm^{-1} (points 1 and 4 on the spectrum) nearly disappeared. This can be attributed to the leaching effect of the aggressive chloride solutions.

Also, the formation of new S-O stretch bands is identified at 953 and 1135 cm^{-1} in case of NC-NS and MC-MS, respectively. This can be interpreted as the formation of ettringite in case of NC-NS, and with denser concentrations in MC-MS referring to the formation of hydrated magnesium silicate, which is characterized by having no bonding ability. Points 2, 3, 5 and 6 (711, 874, 1385 and 1430 cm^{-1}) show loss of calcite in the OPC. This may have resulted from the higher porosity of the concrete and consequently the leach of portlandite. Points 7 and 8 (1633 and 3470 cm^{-1}) refer to the loss of crystalline water in OPC concrete leading to higher permeability and loss of strength [21].

In relation to S+5%MK, and after comparing the spectra of the sample in TW with NC-NS and MC-MS, the following characteristics are observed: the gain of Si-O bond in geopolymer matrix as the band of 450 and 1003cm^{-1} (points 1 and 3 on the spectrum) enhances in MC-MS due to the use of high ratio of Na_2SiO_3 in the activator solution [29] and boosts in NC-NS. This can be attributed to the activation effect of the NC-NS media [22, 23]. Points 2, 4 and 5 (874, 1385 and 1420 cm^{-1}) show formation of sodium and magnesium carbonate in the geopolymer matrix. This may have resulted from the reaction between the aggressive media with lime in the geopolymer. Points 6 and 7 (1633 and 3470 cm^{-1}) refer to the denser formation of crystalline water in geopolymer leading to lower permeability and gain of strength [30].

3.3.2 Scanning electron microscopy (SEM)

After the immersion of OPC and S+5%MK samples in different media for 90 days. The samples are tested in compression and the crushed pieces, which have thin-flat surfaces, are collected and scanned using SEM. Figure 9-a shows the microstructure of the OPC sample immersed in TW for 90 days. The hydration compounds are clear:

CH appears as hexagonal crystals, calcium silicate hydrate as gel, ettringite as needles in addition to an obvious number of voids. In relation to, NC-NS and MC-MS (Fig. 9-b. and Fig. 9-c.) most of portlandite is decomposed and is turned into gypsum and sodium and magnesium silicate hydrate. Moreover, ettringite density increases, and the porosity is remarkably decreased causing internal pressures and formation of micro cracks as a result [21].
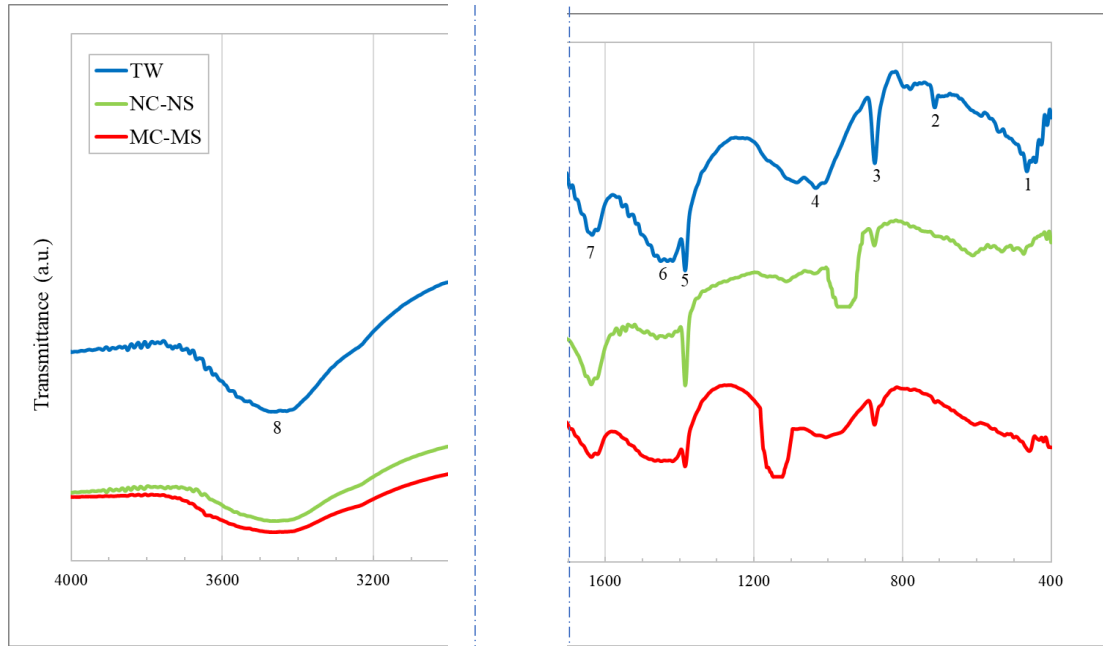

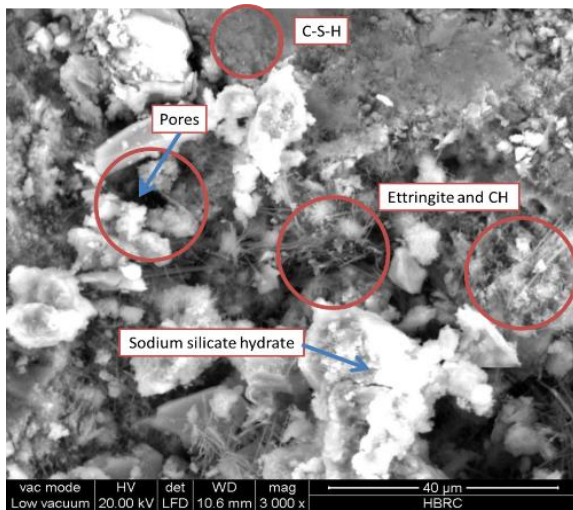Fig. 7. FTIR of OPC samples after 90 days of immersion in different media.
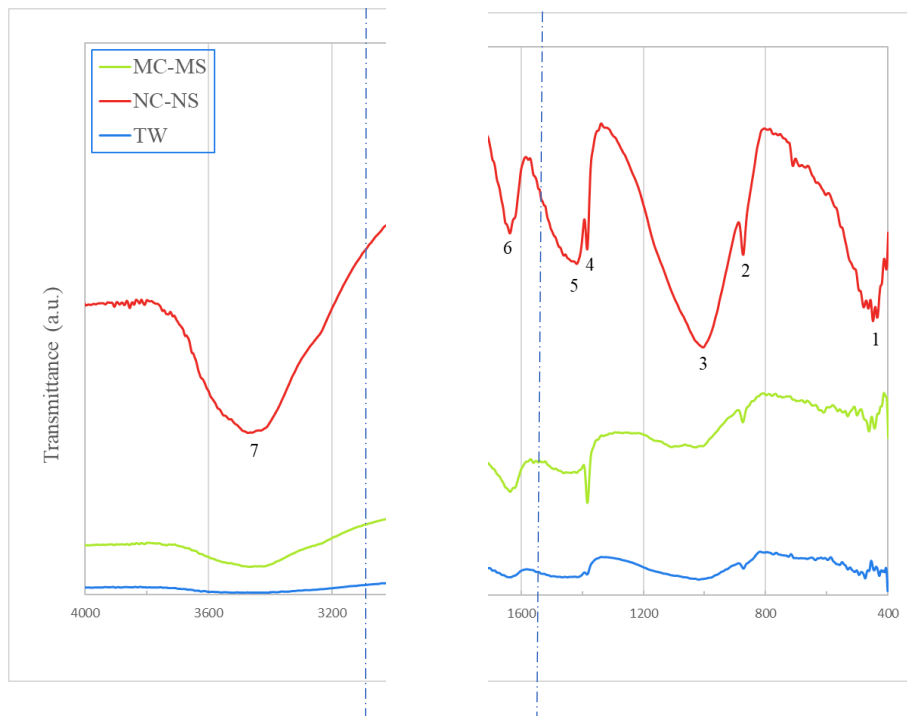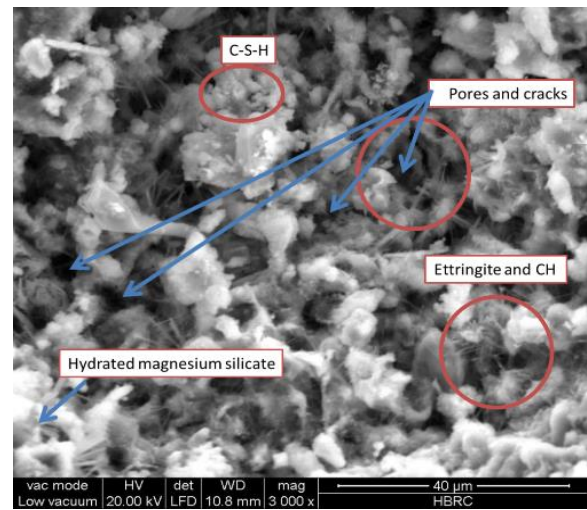

Fig. 8. FTIR of S+5%MK samples after 90 days of immersion in different Media.
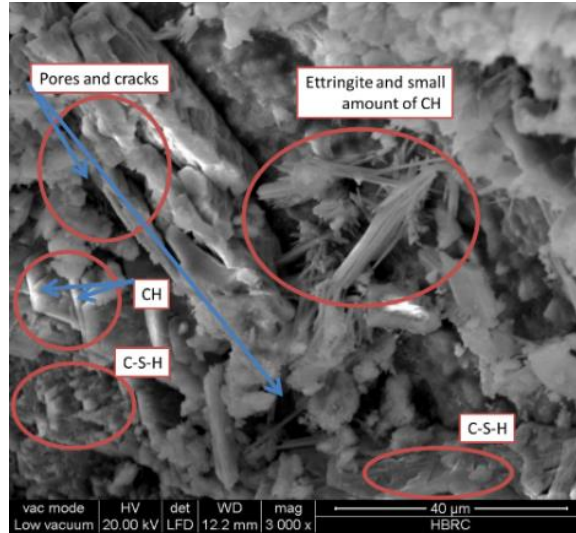
a- TW

b- NC-NS   c- MC-MS

Fig. 9. SEM of OPC samples after 90 days of immersion in different media.

Figure 10-a shows the microstructure of the S+5%MK sample immersed in TW for 90 days. The gel structure of geopolymer is obvious. This can be explained that the use of NaOH causes the formation of stronger bonds between Al and Si in geopolymer matrix. Moreover, the use of Na_2SiO_3 solution provides more free silicates, which increases the density of the geopolymer and strengthens the bonds between Si, O, and Al. The denser geopolymer structure means higher mechanical and more robust physical characteristics. Also, the plate-like elements in the SEM can be interpreted as unreacted MK, which resulted from the inhomogeneous mixing of the ingredients. Moreover, pores can be observed with far lower amounts than in OPC [24].

Figure 10-b shows the effect of NC-NS on geopolymer matrix after 90 days of immersion. Sodium sulphate deposits can be observed. This resulted from the seepage of sodium ions in the matrix. Moreover, the partial transformation of the structure from amorphous to crystalline is obvious. This can be attributed to the duration of immersion, and it can be the reason of the higher compressive strength of the samples after the period of exposure [20]. Figure 10-c shows the effect of MC-MS on geopolymer matrix after 90 days of immersion. The leak of magnesium ions into the matrix can be noticed, and this leads to the formation of Si-Al gel with some Mg to appear intermittently in the matrix. However, this change in the gel seems to have no considerable effect on its strength [20].
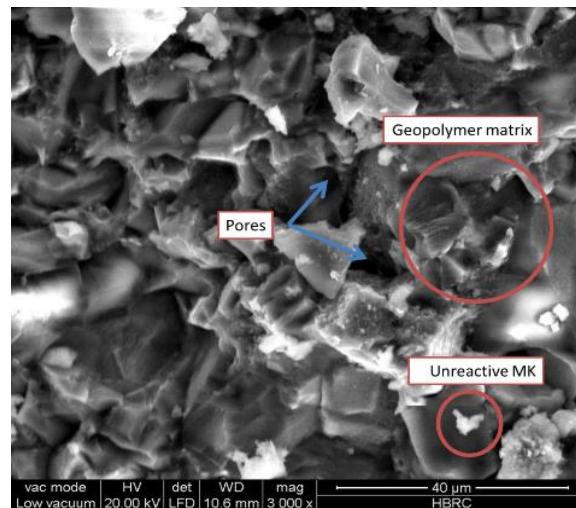
a- TW
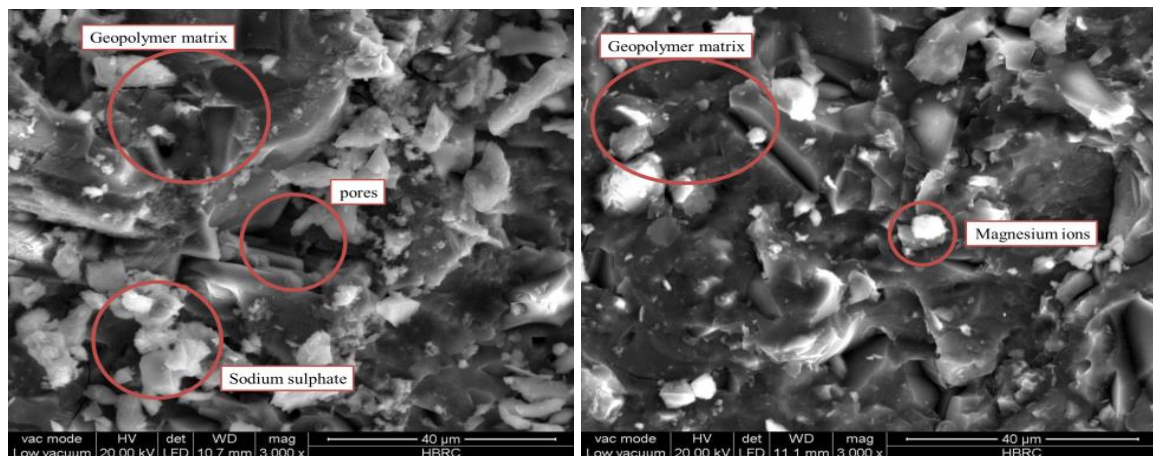
b- NC-NS   c- MC-MS

Fig. 10. SEM of S+5%MK samples after 90 days of immersion in different media.

4. CONCLUSIONS

The high durability of slag with meta-kaolin based geopolymer in sulphate and chloride aggressive media is addressed. Adding meta-kaolin as a partial replacement of slag by a ratio of 5% to the geopolymer mix enhances its compressive strength by about 12%. Moreover, immersion in aggressive media improves geopolymer compressive strength by ratios up to 30%, and the corrosion rate for steel bars significantly decreases. It is concluded that the chemical performance of the geopolymer matrix in the aggressive media is totally different from that of Portland cement. The absence of portlandite and the low amount of calcium in geopolymer make it more durable than conventional Portland cement mixes.

DECLARATION OF CONFLICT OF INTERESTS

The authors have declared no conflict of interests.

REFERENCES

1. Siti, M. S., Al Bakri, A. M., Kamarudin, H., Ruzaidi, C. M., Binhussain, M. and Zaliha, S. Z., "Review on Current Geopolymer as a Coating Material", Australian Journal of Basic and Applied Sciences, Vol. 7, No. 5, pp. 246-257, 2013.
2. http://www.geopolymer.org/applications/ geopolymer-cement, (Accessed 23/12/2017).
3. Davidovits, J., "Geopolymer Cement, a Review", Geopolymer Science and Technics, Geopolymer Institute Library, Technical Paper No. 21, 2013.
4. https://www.fhwa.dot.gov/pavement/concrete/pubs/ hif10014/hif10014. pdf, (Accessed 18/11/2018).
5. Hanjitsuwan, S., Hunpratub, S., Thongbai, P., Maensiri, S., Sata, V., and Chindaprasirt, P., "Effects of NaOH Concentrations on Physical and Electrical Properties of High Calcium Fly Ash Geopolymer Paste", Cement and Concrete Composites, Vol. 45, pp. 9-14, 2014.
6. Gharzouni, A., Samet, B., Baklouti, S., Joussein, E. and Rossignol, S., "Addition of Low Reactive Clay into Metakaolin-Based Geopolymer Formulation: Synthesis, Existence Domains and Properties", Powder Technology, Vol. 288, pp. 212-220, 2016.
7. Provis, J., Palomo, A., and Shi, C., "Advances in Understanding Alkali-Activated Materials", Cement and Concrete Research, Vol. 78, pp. 110-125, 2015.
8. Ye, N., Yang, J., Liang, S., Hu, Y., Hu, J., Xiao, B., and Huang, Q., "Synthesis and Strength Optimization of One-Part Geopolymer Based on Red Mud", Construction and Building Materials, Vol. 111, pp. 317-325, 2016.

9.   Adak, D., Sarkar, M., and Mandal, S., "Effect of Nano-Silica on Strength and Durability of Fly Ash Based Geopolymer Mortar", Construction and Building Materials, Vol. 70, pp. 453-459, 2014.

10.   Haq, E., Padmanabhan, S., and Licciulli, A., "Synthesis and Characteristics of Fly Ash and Bottom Ash Based Geopolymers–A Comparative Study", Ceramics International, Vol. 40, pp. 2965-2971, 2014.

11.   Nazari, A., and Sanjayan, J., "Synthesis of Geopolymer from Industrial Wastes", Journal of Cleaner Production, Vol. 99, pp. 297-304, 2015.

12.   Xie, T., and Ozbakkaloglu, T., "Behavior of Low-Calcium Fly and Bottom Ash-Based Geopolymer Concrete Cured at Ambient Temperature", Ceramics International, Vol. 41, pp. 5945-5958, 2015.

13.   Kannapiran, K., Sujatha, T., and Nagan, S., "Resistance of Reinforced Geopolymer Concrete Beams to Acid and Chloride Migration", Asian Journal of Civil Engineering, Vol. 14, No. 2, pp. 225-238, 2013.

14.   Thokchom, S., Ghosh, P., and Ghosh, S., "Performance of Fly Ash Based Geopolymer Mortars in Sulphate Solution", Journal of Engineering Science and Technology Review, Vol. 3, No. 1, pp. 36-40, 2010.

15.   Deja, J., and Malolepszy, J., "Resistance of Alkali-Activated Slag Mortars to Chloride Solution", 3rd International Conference on the Use of Fly Ash, Silica Fume, Slag and Natural Pozzolans in Concrete, ACI SP, Vol. 114, pp. 1547‑1561, 1989.

16.   Deja, J., and Malolepszy, J., "Long-Term Resistance of Alkali-Activated Slag Mortars to Chloride Solution", 3rd CANMET/ACI International Conference on durability of concrete, Nice, France, (Supplementary Paper), pp. 657‑671, 1994.

17.   Kurdowski, W., Duszak, S., and Trybalska, B., "Corrosion of Slag Cement in Strong Chloride Solutions", 1st International Conference on Alkaline Cements and Concretes, Kiev, Ukraine, Vol. 2, pp. 961‑970, 1994.

18.   Bakharev, T., Sanjayan, J. G., and Cheng, Y. B., "Sulphate Attack on Alkali Activated Slag Concrete", Cement and Concrete Research, Vol. 32, No. 2, pp. 211‑216, 2002.

19.   Abd El-moatey, A., Faried, A., Soufi, W., and Abd El-Aziz, M., "Improve the Formation of Geopolymer Concrete Mixed with Seawater and without Curing", American Journal of Construction and Building Materials, Vol. 2, No. 4, pp. 78-85, 2017.

20.   Provis, J., and Deventer, J., "Geopolymers Structure, Processing, Properties and Industrial Applications", CRC Press, 2009.

21.   Neville, A. M., and Brooks, J. J., "Concrete Technology", 2nd Edition, Pearson Education, 2010.

22.   Hakkinen, T., "Properties of Alkali-Activated Slag Concrete", VTT Research, Technical Research Centre of Finland (VTT), Vol. 540, 1986.

23.   Hakkinen, T., "Durability of Alkali-Activated Slag Concrete", Nordic Concrete Research, Vol. 6, pp. 81‑94, 1987.

24.   Shi, C., Krivenko, P., and Roy, D., "Alkali-Activated Cements and Concretes", 1st Edition, CRC Press, 2003.

25. Toutanji, H., Delatte, N., Aggoun, S., Duval, R., and Danson, A., "Effect of Supplementary Cementitious Materials on the Compressive Strength and Durability of Short-Term Cured Concrete", Cement and Concrete Research, Vol. 34, No. 2, 2004.

26. Kong, D., and Sanjayan, J., "Effect of Elevated Temperatures on Geopolymer Paste, Mortar and Concrete", Cement and Concrete Research, Vol. 40, pp.334-339, 2010.

27. McCaffrey, R., "Climate Change and the Cement Industry", Global Cement and Lime Magazine: Environmental Special Issue, pp. 15-19, 2002.

28. Hanna, R. A., Barrie, P. J., Cheeseman, C. R., Hills, C. D., Buchler, P. M., and Perry, R., "Solid State 29Si and 27Al NMR and FTIR Study of Cement Pastes Containing Industrial Wastes and Organic" Cement Concrete Research, Vol. 25, pp.1435-1444, 1995.

29. Krivenko, P. V., "Synthesis of Cementitious Materials in a System R_2O-Al_2O_3-SiO_2-H_2O with Required Properties", D.Sc. (Eng.) Thesis, Kiev Civil Engineering Institute, Kiev, Ukraine, 1986.

30. Donatello, S., Palomo, A., and Fernandes-Jimenez, A., "Durability of Very High Volume Fly Ash Cement Pastes and Mortars in Aggressive Solutions", Cement and Concrete Composition, Vol. 38, pp. 12-20, 2013.

المتانة ومقاومة تآكل حديد التسليح للخرسانة الجيوبوليمرية المكونة من الخبث والميتاكاولين

يدرس البحث أداء الخرسانة الجيوبوليمرية المكونة من الخبث والميتاكاولين تحت تأثير الأوساط المهاجمة لها حيث تمت دراسة تأثير إضافة الميتاكاولين على مقاومة الضغط للخرسانة الجيوبوليمرية المكونة من الخبث و تجهيز عينات مونة وخرسانة من الأسمنت البورتلاندي العادي والجيوبوليمر وغمرها في الماء والأوساط المهاجمة لها ٩٠ يوم لتحديد متانة العينات باختبارات مقاومة الضغط وطيف الأشعة تحت الحمراء والتصوير بالميكروسكوب الالكتروني ودراسة مقاومة تآكل حديد التسليح بالعينات الخرسانية باختبار مقاومة الاستقطاب الخطي واستنتاج امكانية الوصول لأعلى مقاومة ضغط للخرسانة الجيوبوليمرية بإضافة ٥ % من الميتاكاولين من وزن الخبث حيث تبين أن مقاومة الضغط لعينات الجيوبوليمر تزيد حوالي ٣٠ % في الأوساط المهاجمة بالمقارنة بعينات الجيوبوليمر المعالجة في المياه وأن معدل تآكل الحديد في عينات الجيوبوليمر يكاد يصل للصفر وان التكوين المجهري لعينات الجيوبوليمر يظهر بناء أكثر مقاومة للأوساط المهاجمة بالمقارنة بعينات الأسمنت البورتلاندى.